



Co-activation of Nonselective Cation Channels by Store Depletion and Oxidative Stress in Monocytic U937 Cells

Hui-Fang Li¹, Ai-Yu Shen², Chung-Ren Jan¹ and Sheng-Nan Wu¹

¹*Department of Medical Education and Research
Veterans General Hospital-Kaohsiung
Kaohsiung 813, Taiwan*

²*Department of Pharmaceutical Sciences
Foo-Yin Institute of Technology
Kaohsiung 831, Taiwan, ROC*

Abstract

Two different types of nonselective cation currents in monocytic U937 cells were characterized with the aid of patch-clamp technique. When the cells were exposed to oxidative stress with 10 mM H₂O₂, a nonselective cation current (I_{NS}) can be elicited. This current was still observed when extracellular cations are Ca²⁺. The change in intracellular Cl⁻ concentrations did not shift the reversal potential of this current. This current showed no any rectification, and was time- and voltage-independent at any potentials. The further addition of LaCl₃ (100 μM) or dithiothreitol (10 μM) effectively suppressed this current. However, SK & F 96365 (100 μM) or nifedipine (10 μM) did not produce any effect on it significantly. On the other hand, depletion of Ca²⁺ stores by different maneuvers, such as the application of ATP, thapsigargin or A23187, or dialysis of the cells with inositol-1,4,5-trisphosphate activated another type of nonselective current which was identified as store-operated Ca²⁺-permeable current (I_{SOC}). Unlike H₂O₂-induced I_{NS}, this current was observed to slowly inactivate when the voltage steps were hyperpolarized. Current-voltage relation of this current showed inward rectification. When the cell was challenged with both store depletion and H₂O₂, I_{NS} on the top of I_{SOC} can be activated. These results suggest that different types of nonselective cation channels can be co-expressed in the same cell. Therefore, in U937 cells nonselective cation currents can be activated after the stimulation with oxidative stress, store depletion or both. The activation of these nonselective cation channels may affect intracellular Ca²⁺ homeostasis.

Key Words: monocyte, nonselective cation current, oxidative stress

Introduction

The increase in cytosolic Ca²⁺ concentrations can be induced by chemical injuries associated with oxidative stress. Oxidative injury may be linked with the oxidation of sulfhydryl groups on Ca²⁺-ATPase in the cell (6, 21, 22). A previous study showed that Ca²⁺ release channels from the sarcoplasmic reticulum of skeletal muscle can be activated by the oxidation of critical thio-containing residues (22). In addition, Ca²⁺ ions may enter through ion channels or through pores opened by damage to the cell membrane. On the other hand, the rise in cytosolic Ca²⁺ concentrations

may be an epiphenomenon that occurs in association with the loss of cell viability, so that the cell membrane becomes physically disrupted and extracellular Ca²⁺ ions then pass into the cytosol of an already irreversibly damaged cells (6, 24).

The activation of nonselective cation channels elicited by oxidative stress has recently been demonstrated in several nonexcitable cell types; including endothelial cells and adipocytes (11, 12, 17). Monocytes represent the circulating members of the mononuclear phagocyte system, and they can readily suffer from oxidative stress and also be activated with the production of H₂O₂. However,

little information is available for ionic mechanisms of oxidative injury with the challenging of H_2O_2 in monocytes. Previous observation at our laboratory ever showed that monocytic U937 cells possessed a unique type of store-operated Ca^{2+} -permeable channel which is responsive to dihydropyridine compounds (28). Several reports also suggested that the activation of these channels may lead to a significant Ca^{2+} influx which is related to cell proliferation or differentiation (4, 14, 15, 27). Furthermore, this cell line has been considered to be a good model for the study of monocyte differentiation or mitogenesis (4, 7, 27). Therefore, the main objective of the present study is the identification of different types of nonselective cation channels in U937 cells, and to provide evidence that the currents induced by oxidative injury and store depletion are different.

Materials and Methods

Preparation of Cells

Monocytic U937 cells were grown in RPMI 1640 (Gibco, Grand Island, NY) supplemented with 10% fetal calf serum (Gibco) and 100 U/ml penicillin, 100 μ g/ml streptomycin (Sigma Chemicals, St. Louis, MO), 5 mM glucose and 24 mM $NaHCO_3$. Cells were incubated at 37 °C in a CO_2/O_2 :5%/95% atmosphere, and were maintained in culture prior to use (7, 28). Cell viability was always assessed by the trypan blue dye-exclusion test.

Electrophysiological Measurement

U937 cells were transferred to a recording chamber which was mounted on the stage of an inverted phase-contrast microscope (Diaphot-200; Nikon, Tokyo, Japan). The microscope was coupled to 1500X in order to monitor the changes of cell size. Ionic currents were recorded with glass pipettes in the whole-cell voltage-clamp amplifier (RK-400; Biologic, Claix, France) (1, 5, 28). The patch pipettes were made from the capillary tubes (Kimax-51; Kimble Products, Vineland, NJ) using a vertical two-step electrode puller (PB-7; Narishige, Tokyo, Japan). The resistance of the patch pipette was 3-5 M Ω when it was immersed in normal Tyrode's solution. A hydraulic micromanipulator (WR-6; Narishige) which was mounted on the fixed stage of an inverted microscope was used to position the pipette near the cell. In experiments designed to construct the current versus voltage (I-V) relationships, either square command pulses with a duration of 1 sec from holding potential to various potentials or linear ramp pulses with a duration of 200 msec from -90 mV to +40 mV

were used. The square or ramp voltage-step command signals were digitally generated by a programmable stimulator (SMP-311; Biologic).

Data Recording and Analysis

The signals consisting of voltage and current tracings were monitored on a digital storage oscilloscope (model 1602; Gould, Valley View, OH) and on-line recorded onto digital tapes by using a digital audio tape recorder (model 1204; Biologic). After the experiments were performed, the stored data were then fed back and digitized at the sampling frequency of 5-10 kHz with a DigiData 1200 series interface (Axon Instruments, Foster City, CA) which was controlled by pClamp 6.03 software package (Axon Instruments). To measure inhibition of each agent on I_{NS} , the amplitude of inward current at the level of -80 mV was taken to be 1.0 and the relative amplitude of I_{NS} after the further application of each agent was then compared. The inactivation time course of nonselective cation current induced by store depletion was fitted by one exponential model.

All data were reported as mean \pm standard error of mean (S.E.M.). The paired or unpaired Student's t test and Duncan's multiple range test were used for the statistical analyses. The level of significance was taken by $p < 0.05$.

Drugs and Solutions

Adenosine-5'-triphosphate, guanosine-5'-triphosphate, dithiothreitol, nifedipine, A23187, hydrogen peroxide (H_2O_2) and t-butyl hydroperoxide were purchased from Sigma Chemicals (St. Louis, MO). Inositol-1,4,5-trisphosphate hexasodium (IP_3), thapsigargin and SK&F 96365 (1- β -[3-(4- β -methoxyphenyl) propoxy]-4-methoxyphen ethyl]-1H-imidazole hydrochloride) were purchased from Research Biochemicals (Natick, MA). All other chemicals we obtained from regular commercial chemicals and were of reagent grade. The composition of normal Tyrode's solution was as follows (in mM): NaCl 136.5, KCl 5.4, $CaCl_2$ 1.8, $MgCl_2$ 0.53, glucose 5.5 and HEPES-NaOH buffer 5.5 (pH 7.4). The patch pipette was filled with solution (in mM): Cs-aspartate 130, CsCl 20, $MgCl_2$ 1, EGTA 0.1, Na_2ATP 3, Na_2GTP 0.1 and HEPES-CsOH buffer (pH 7.2). To measure K^+ currents or membrane potential, Cs^+ ions inside the pipette solution were replaced with equimolar K^+ ions, and the pH was adjusted to 7.2 with KOH. In some experiments, IP_3 (10 μ M) was added to the pipette solution in order to cause the emptying of IP_3 -sensitive Ca^{2+} stores.

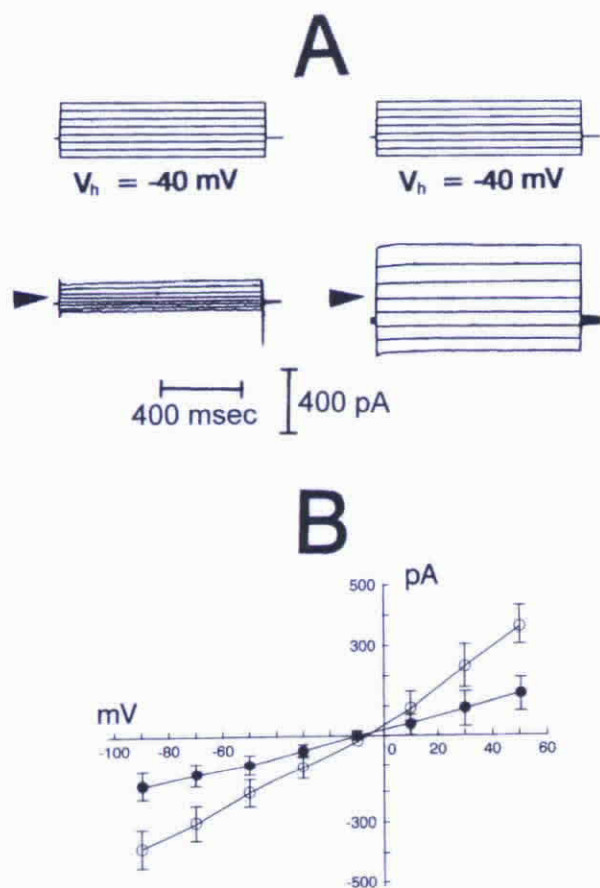


Fig. 1. Activation of a nonselective cation current during oxidant stress by exposing a cell to H_2O_2 . The patch pipette contained Cs^+ solution to block K^+ channels. The superimposed voltage and current traces were shown in upper and lower parts of panel A, respectively. The holding potential (V_h) was set at -40 mV and various voltage steps with a duration of 1 sec at 0.1 Hz were then applied. The arrows shown in left side of current traces indicate the zero current level. The voltage and current traces shown in left side are control and those in right side were recorded 5 min after the presence of H_2O_2 (10 mM). Panel B shows the current versus voltage (I-V) relationships in the absence (●) and presence (○) of H_2O_2 (10 mM). Each data point shown in right side of each panel is the mean \pm S.E.M. of five to seven cells.

Results

Activation of a non selective cation current by H_2O_2

The whole-cell configuration of the patch-clamp technique was carried out to measure ionic currents. The experiments shown in the present study were mostly conducted with the pipette solution containing 130 Cs-aspartate, 20 mM CsCl, 3 mM Na_2ATP and 0.1 mM GTP. Figure 1 shows an example of a cell challenged with the presence of 10 mM H_2O_2 , in which ionic currents were measured when patch pipette was filled with Cs^+ -containing solution. When the cells were held at the level of -40 mV, voltage steps (from -90 to $+50$ mV, increment 20 mV) elicited only

small currents in resting cells, but much larger currents during the application of H_2O_2 (10 mM). For example, at the level of $+50$ mV, H_2O_2 caused a significant increase of membrane currents from 136 ± 51 pA to 358 ± 63 pA ($n = 6$ cells). However, no significant difference can be demonstrated at -10 mV between the absence and presence of H_2O_2 (-9 ± 12 pA versus -13 ± 0 pA; $n = 6$ cells). As shown in Figure 1B, these currents show little rectification and are time-independent. The same response was also observed when the cells were exposed to t-butyl hydroperoxide (1 mM). The reversal potential of H_2O_2 -induced current was -3 ± 1 mV ($n = 5$ cells) and was not significantly shifted by the change in intracellular Cl^- concentrations. These results suggest that the exposure of H_2O_2 to cells can activate a nonselective cation current (I_{NS}), but not Cl^- current in this condition (1).

The effects of $LaCl_3$, $NiCl_2$, SK&F 96365 and nifedipine on H_2O_2 -elicited I_{NS} in U937 cells were also investigated. As shown in Figure 2, SK&F 96365 or nifedipine did not abolish H_2O_2 -elicited current, whereas $LaCl_3$ (100 μM) or dithiothreitol (10 μM) can effectively suppress this current. When extra cellular Na^+ was replaced by Ca^{2+} , the presence of H_2O_2 still activated this current. Thus, Ca^{2+} is also the charge carrier for H_2O_2 -induced current. It is likely that the challenging of the cell with H_2O_2 can elicit a nonselective cation channel which is permeable to Na^+ , K^+ , Cs^+ and Ca^{2+} in U937 cells.

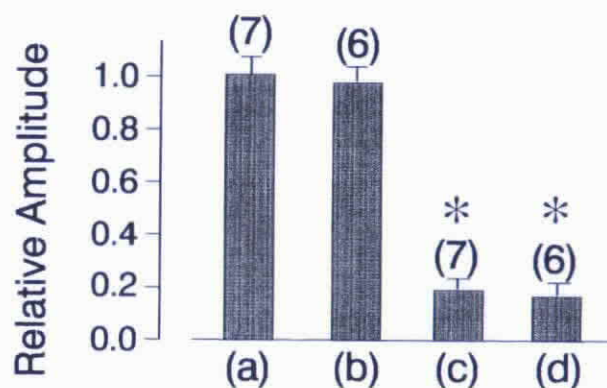


Fig. 2. Comparison among the effects of $LaCl_3$, dithiothreitol, SK&F 96365 and nifedipine on the amplitude of I_{NS} elicited by the presence of oxidative stress with H_2O_2 in U937 cells. Each cell was held at the level of -40 mV, and the 200-msec ramp pulses from -90 and $+40$ mV at a rate of 0.1 Hz were applied. The amplitude of I_{NS} at -80 mV after the presence of H_2O_2 (10 mM) was considered to be 1.0 and the relative amplitude of I_{NS} after the further application of each agent was then plotted. The parentheses denote the number of cells examined. Mean \pm S.E.M.. (a): 10 μM nifedipine; (b): 100 μM SK&F 96365; (c) 100 μM $LaCl_3$; (d) 10 μM dithiothreitol. *indicates significant difference from control group, i.e., the presence of H_2O_2 alone.

Depletion of Ca^{2+} Stores Activates a Nonselective Current

Stimulating U937 cells with ATP in normal Tyrode's solution activates a membrane current which is closely correlated with the depletion of Ca^{2+} stores. Figure 3 shows current responses in whole-cell mode from a cell that was clamped at -40 mV during voltage ramp protocols repetitively applied throughout the whole experiment. Figure 3A shows the time course of the current amplitudes measured at $+40$ and -80 mV. The I-V curves before and during the application of ATP ($100 \mu\text{M}$) are shown in Figure 3B. The inwardly rectifying current component, which is present in the majority of the cells, has also been identified as a nonselective cation current which is Ca^{2+} -permeable. Alteration of extracellular or intracellular chloride concentration did not shift the reversal potential.

Gating of this current should not be due to a ligand-dependent mechanism but to the emptying of Ca^{2+} stores, because it can also be activated by loading

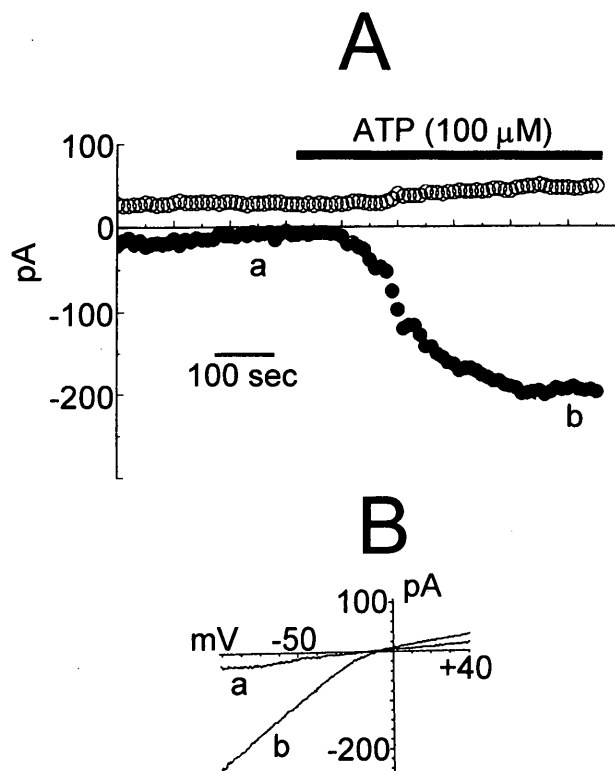


Fig. 3. Activation of a nonselective cation current by the application of ATP. The patch pipette was loaded with Cs^+ containing solution and cells were bathed in normal Tyrode's solution containing 1.8 mM CaCl_2 . The cell was held at the level of -40 mV, and the linear ramp pulses from -90 to $+40$ mV with a duration of 200 msec at a rate of 0.1 Hz were then applied. Panel A shows the time course in the change of current amplitudes measured at $+40$ mV (\circ) and -80 mV (\bullet). The bar shown in the upper part denotes the application of ATP ($100 \mu\text{M}$). In panel B, current versus voltage (I-V) relations were plotted from voltage ramps marked by the labels (a and b) in panel A.

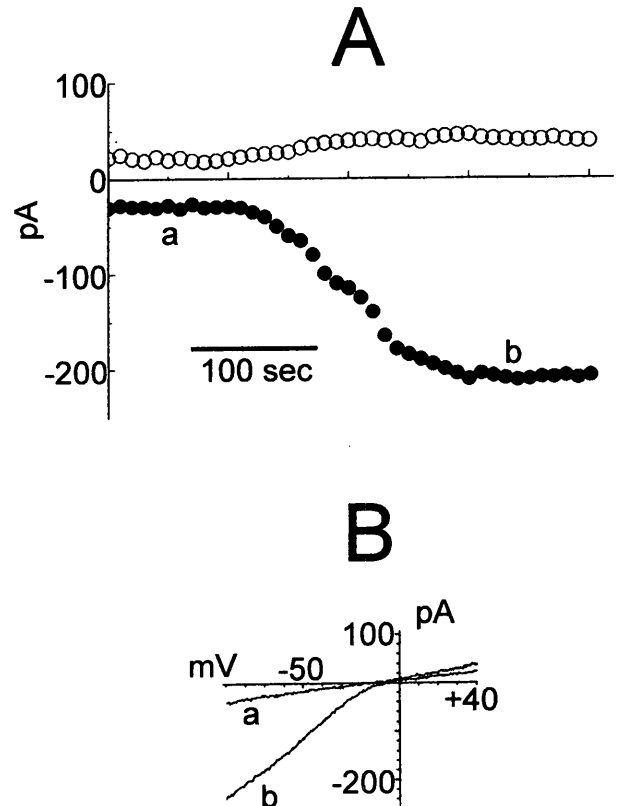


Fig. 4. Activation of a nonselective cation current with intracellular dialysis with inositol triphosphate. The patch pipette was loaded with Cs^+ containing solution and cells were bathed in normal Tyrode's solution containing 1.8 mM CaCl_2 . The cell was held at the level of -40 mV, and the linear ramp pulses from -90 to $+40$ mV with a duration of 200 msec at a rate of 0.1 Hz were then applied. Panel A shows the time course in the changes of membrane currents after breaking into a cell with a pipette solution containing IP_3 ($10 \mu\text{M}$). Current amplitudes at $+40$ mV (\circ) and -80 mV (\bullet) were obtained from the voltage ramp protocol. In panel B, current versus voltage (I-V) relations were plotted from voltage ramps marked by the labels (a and b) in panel A.

the cell via the patch pipette with IP_3 ($10 \mu\text{M}$). As shown in Figure 4, membrane currents were immediately measured after the rupture of membrane patch. When the cell membrane was ruptured, cytosolic IP_3 was elevated due to diffusion of the pipette solution containing $10 \mu\text{M}$ IP_3 into the cytoplasm. Figure 4A shows the time course of the corresponding currents at $+40$ and -80 mV from the voltage ramp protocols, as described above. Some representative I-V curves, taken at the times indicated by the labels (a and b), are shown in Figure 4B. Notably, current amplitudes measured during voltage steps initially after breaking the cell membrane were small. Subsequently, the rise in the level of IP_3 activated an inwardly rectifying current which is store-operated Ca^{2+} -permeable current (I_{SOC}) (Figure 4B). Figure 5 shows some characteristic features of I_{SOC} . Voltage steps (from -40 to $+110$ mV, increment 20 mV) evoked only small currents initially, but

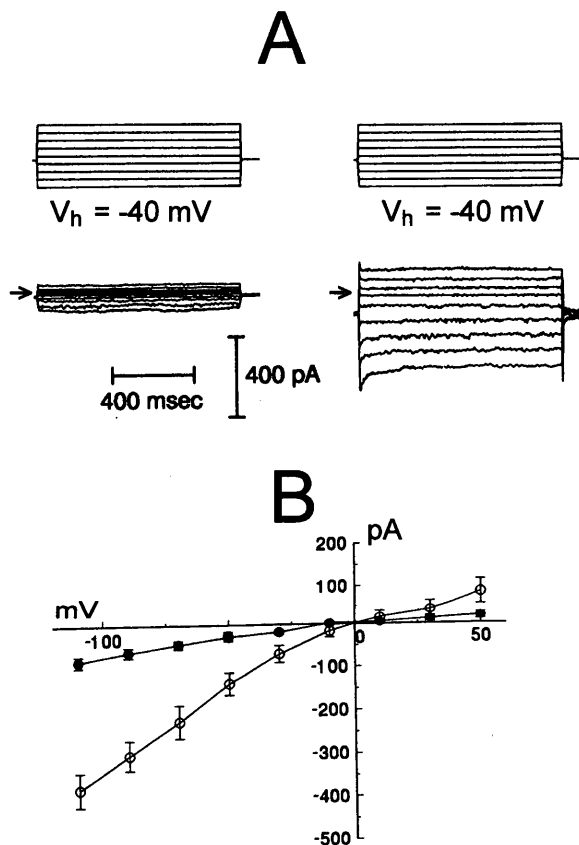


Fig. 5. Characterization of nonselective cation current by store depletion with intracellular dialysis of inositol triphosphate (IP₃). The patch pipette contained Cs⁺ solution and 10 μM IP₃. The superimposed voltage and current traces were shown in upper and lower parts of panel A, respectively. The holding potential (V_h) was set at -40 mV and various voltage steps with a duration of 1 sec at 0.1 Hz were then applied. The arrows shown in left side of current traces indicate the zero current level. Panel B shows the current versus voltage (I-V) relationships in the beginning of membrane rupture (●) and 5 min after intracellular perfusion with IP₃ (○). Each data point shown in right side of each panel is the mean ± S.E.M. of four to seven cells.

much larger current 5 minutes after the rupture of membrane. The individual current traces during the voltage steps were found to exhibit a slow inactivation at negative potentials as shown in previous reports (4, 30). For instance, when the voltage steps from -40 to -110 mV were applied, the current peaked and then inactivated to a new steady-state level with a monoexponential time constant of 84 ± 7 msec (n = 5 cells). The amount of inactivation was increased with the size of voltage step. Moreover, this current is voltage-dependent and resembles the current which is activated by application of ATP. Likewise, these results were also obtained if Ca²⁺ stores were depleted by another maneuvers where the cells were exposed to thapsigargin (500 nM), an inhibitor of endoplasmic reticulum Ca²⁺-ATPase (20) or A23187 (10 μM). Thus, the activation of this current is

identified as I_{SOCC} which shares similarity to Ca²⁺ release-activated current reported in other cells (2, 9, 10, 16, 19, 30).

Co-activation of Nonselective Cation Currents Induced by H₂O₂ and Store Depletion

Nonselective cation currents activated by H₂O₂ and store depletion can be discriminated on the basis of their different kinetic and rectification properties. Interestingly, these currents are also illustrated in the same cell. As shown in Figure 6, the application of ATP (100 μM) activated a nonselective cation current. At the plateau level of the change in ionic currents, the cell was challenged with H₂O₂ (10 mM). Under this condition, the application of H₂O₂ further activated both inward and outward currents. These currents were virtually time-independent and turned out to be not rectifying. The similar results were also obtained when cells were loaded with IP₃ (10 μM) and H₂O₂ was subsequently applied to the bath. These experiments indicate that two different nonselective currents are able to be co-activated in the majority of

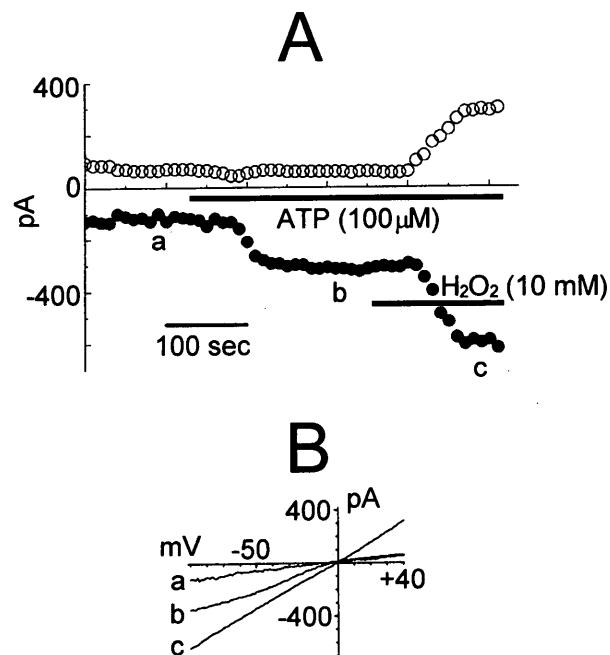


Fig. 6. Two types of nonselective cation currents induced by H₂O₂ and store depletion in the same cells. The cell was held at -40 mV, and the 200-msec ramp pulses from -90 to +40 mV at a rate of 0.1 Hz were then applied. Panel A shows the time course in the changes of membrane currents after the application of ATP (100 μM) and H₂O₂ (10 mM). Current amplitudes at +40 mV (○) and -80 mV (●) were obtained from the voltage ramp protocol. The bars shown in panel A indicate the application of each agent. In panel B, current versus voltage (I-V) relations were obtained from voltage ramps marked by the labels (a, b and c) in panel A. Current trace labeled a is control, labeled b was recorded in the presence of 100 μM ATP, and labeled c was obtained after the addition of H₂O₂ (10 μM) but still in the presence of ATP.

the cells.

Discussion

The results of the present study clearly demonstrate that the monocytic U937 cells express two types of nonselective cation currents (I_{NS}) which are gated by oxidative stress and store depletion. We have also shown that both channel types can co-exist in the same cells. Therefore, a direct comparison between these channel types might be necessary, because not only the activation mechanism of H_2O_2 -induced I_{NS} is unclear, but an H_2O_2 -induced change in the level of oxidized glutathione may be a possible mode of activation as well (12, 13, 18, 24). It has been already shown that the emptying of Ca^{2+} store by different maneuvers can activate nonselective cation current in a variety of cells (10, 16, 19, 23, 25, 30). A few reports demonstrated the activation of nonselective current by oxidative stress (12, 13).

Glutathione, a thiol tripeptide (g-glutamyl-cysteinyl-glycine), is found in most cells where it functions as a reducing agent to keep proteins with critical sulfhydryls (cysteine residues) in the reduced state. Reduced glutathione is able to react with organic peroxides and subsequently converted to oxidized glutathione. Henshke and Elliot (1995) demonstrated that high level of oxidized glutathione inside the cell can reduce capacitative Ca^{2+} influx (8). Because oxidative stress readily affects the integrity of the cell membrane and redox reagents usually react with essential cysteine groups on channel proteins, it is thus possible that the activation of I_{NS} by the challenging with H_2O_2 is related to an increase in the level of oxidized glutathione inside the cells (13, 18). In fact, the present finding showing that the presence of dithiothreitol, a reducing agent to keep glutathione in the reduced state, suppressed H_2O_2 -induced I_{NS} supports this notion. Further work on redox modulation of channel proteins is also interesting to be explored.

By comparison, our finding that the activation of store-operated current requires the emptying of Ca^{2+} stores (28) contrasts with properties of nonselective cation current induced by oxidative injury with H_2O_2 which is not affected by Ca^{2+} concentrations inside internal stores. One of the most striking differences is the stronger inward rectification of the store-operated currents in comparison with the H_2O_2 -elicited currents. Other differences are the slow inactivation of store-operated currents at negative potentials. Pharmacologically, $LaCl_3$ blocked both types of channels, whereas SK&F 96365 and nifedipine did not suppress H_2O_2 -elicited current. However, both SK&F 96365 and

nifedipine can produce an inhibitory effect on the current amplitude induced by store depletion (9, 27, 28).

Our results clearly showed that nonselective cation channels induced by the depletion of Ca^{2+} stores in U937 cells exhibit inward rectification. Similarly, Floto et al reported that Ca^{2+} current activated by depletion of Ca^{2+} stores can be upregulated in differentiated U937 cells (4). Therefore, it is noteworthy that when the cell is depolarized from -40 to near -10 mV, the electrochemical driving force necessary for Ca^{2+} entry will be reduced (14), thereby producing an inhibition of Ca^{2+} influx. In the present study, the stimulation of U937 cells with H_2O_2 resulted in a 30 mV membrane depolarization from -38 to -8 mV, under the conditions in which the activation of nonselective channel occurred. These results can be interpreted to indicate that oxidant-elicited nonselective cation channel is responsible for membrane depolarization and will thus contribute to the inhibition of store-dependent Ca^{2+} influx (8).

It is also likely that Ca^{2+} ions entering through oxidant-activated channels itself can produce the inhibition of store-dependent Ca^{2+} influx. Store-dependent Ca^{2+} channels in mast cells can be inhibited by intracellular Ca^{2+} concentrations in a manner similar to L-type voltage-gated Ca^{2+} channels (3, 29, 30). Because such an effect occurs on a millisecond time scale, it is believed to be a direct effect of Ca^{2+} on the channel (29). On the other hand, in non-excitable cells like U937 cells, a slower, Ca^{2+} -dependent inhibition of Ca^{2+} influx may be due to the fact that the refilling of Ca^{2+} stores develops. The present studies show that the oxidant-activated channel is also able to conduct inward Ca^{2+} current. It is thus likely that Ca^{2+} influx through oxidant-elicited nonselective cation channel with the resultant elevation of intracellular Ca^{2+} concentrations in localized regions beneath the plasma membrane leads to the inhibition of store-dependent Ca^{2+} entry (26).

In summary, monocytic U937 cells express nonselective cation channels induced by oxidative injury or store depletion. The present study further presents the finding that two nonselective cation channels co-exist. Each of these classes of nonselective cation channels is supposed to be predominantly activated by its specific stimulus, store depletion or oxidative injury inducing damage in surface membrane, but they might also become co-activated under various physiological conditions. However, further investigation should be done to determine whether the modulation of the activity in these two channels plays a role in the immunological functions of these cells.

Acknowledgments

The authors would like to thank Dr. Ming-Hong Tai for providing U937 cells. This work was partly supported by grants from National Science Council (NSC-87-2314-B-075B-013) and Kaohsiung-Veterans General Hospital (VGHKS-87-52), Taiwan, ROC.

References

1. Chou, C.Y., M.R. Shen and S.N. Wu. Volume-sensitive chloride channels associated with human cervical carcinogenesis. *Cancer Res.* 55: 6077-6083, 1995.
2. Delles, C.T., T. Haller and P. Dietl. A highly calcium-selective cation current activated by intracellular calcium release in MDCK cells. *J. Physiol.* 486: 557-567, 1995.
3. Fabiato, A. Time and calcium dependence of activation and inactivation of calcium-induced release of calcium from the sarcoplasmic reticulum of a skinned canine cardiac Purkinje cell. *J. Gen. Physiol.* 85: 247-289, 1985.
4. Floto, R.A., M.P. Mahaut-Smith, J.M. Allen and B. Somasundaram. Differentiation of the human monocytic cell line U937 results in an upregulation of the calcium release-activated current, ICRAC. *J. Physiol.* 495: 331-338, 1996.
5. Hamill, O.P., A. Marty, E. Neher, B. Sakmann and F.J. Sigworth. Improved patch-clamp techniques for high-resolution current recording from cells and cell-free membrane patches. *Pflügers Arch.* 391: 85-100, 1981.
6. Harman, A.W. and M.J. Maxwell. An evaluation of the role of calcium in cell injury. *Annu. Rev. Immunol. Toxicol.* 35: 129-144, 1995.
7. Harris, P. and P. Ralph. Human leukemic models of myelomonocyte development: a review of the HL60 and U937 cell lines. *J. Leukocyte Biol.* 37: 407-422, 1985.
8. Henshke, P.N. and S.J. Elliott. Oxidized glutathione decreases luminal Ca^{2+} content of the endothelial cell $Ins(1,4,5)P_3$ -sensitive Ca^{2+} store. *Biochem. J.* 312: 485-489, 1995.
9. Hopf, F.W., P. Reddy, J. Hong and R.A. Steinhardt. A capacitative calcium current in cultured skeletal muscle cells is mediated by calcium-specific leak channel and inhibited by dihydropyridine compounds. *J. Biol. Chem.* 271: 22358-22367, 1996.
10. Hoth, M. and R. Penner. Calcium release-activated calcium current in rat mast cells. *J. Physiol.* 465: 359-386, 1993.
11. Koivisto, A., D. Siemen and J. Nedergaard. Reversible blockade of the calcium-activated non-selective cation channel in brown fat cells by the sulfhydryl reagents mercury and thimerosal. *Pflügers Arch.* 425: 549-551, 1993.
12. Koliwad, S.K., D.L. Kunze and S.J. Elliott. Oxidant stress activates a non-selective cation channel responsible for membrane depolarization in calf vascular endothelial cells. *J. Physiol.* 491:1-12, 1996.
13. Koliwad, S.K., S.J. Elliott and D.L. Kunze. Oxidized glutathione mediates cation channel activation in calf vascular endothelial cells during oxidant stress. *J. Physiol.* 495: 37-49, 1996.
14. Liu, S.I., C.W. Chi, W.Y. Lui, K.T. Mok, C.W. Wu and S.N. Wu. Correlation of hepatocyte growth factor-induced proliferation and calcium-activated potassium current in human gastric cancer cells. *Biochim. Biophys. Acta.* 1368 : 256-266, 1998.
15. Lovisolò, D., C. Distasi, S. Antoniotti and L. Munaron. Mitogens and calcium channels. *Trends Physiol. Sci.* 12: 279-285, 1997.
16. L(ckhoff, A and D.E. Clapham. Calcium channels activated by depletion of internal calcium stores in A431 cells. *Biophys. J.* 67: 177-182, 1994.
17. Nilius, B. Permeation properties of a non-selective cation channel in human vascular endothelial cells. *Pflügers Arch.* 416: 609-611, 1990.
18. Ochi, T. Mechanism for the changes in the levels of glutathione upon exposure of cultured mammalian cells to tertiary-butylhydroperoxide and diamide. *Arch. Toxicol.* 67: 401-410, 1993.
19. Popp, R. and H. Gogelein. A calcium and ATP sensitive nonselective cation channel in the antiluminal membrane of rat cerebral capillary endothelial cells. *Biochim. Biophys. Acta.* 1108: 59-66, 1992.
20. Premack, B.A., T.V. McDonald and P. Gardner. Activation of Ca^{2+} current in Jurkat T cells following the depletion of Ca^{2+} stores by microsomal Ca^{2+} -ATPase inhibitors. *J. Immunol.* 152: 5226-5240, 1994.
21. Sakagami, H., N. Kuribayashi, M. Iida, T. Hagiwara, H. Takahashi, H. Yoshida, F. Shiota and H. Ohata. The requirement for and mobilization of calcium during induction by sodium ascorbate and by hydrogen peroxide of cell death. *Life Sci.* 58: 1131-1138, 1996.
22. Salama, G., J.J. Abramson and G.K. Pike. Sulfhydryl reagents trigger Ca^{2+} release from the sarcoplasmic reticulum of skinned rabbit psoas fibres. *J. Physiol.* 454: 389-420, 1992.
23. Skutella, M. and U.T. Rüegg. Increase in empty pool-activated Ca^{2+} influx using an intracellular Ca^{2+} chelating agent. *Biochem. Biophys. Res. Comm.* 218 : 837-841, 1996.
24. Suzuki, Y.J., H.J. Horman and A. Sevanian. Oxidant as stimulators of signal transduction. *Free Radical Biol. Med.* 22: 269-285, 1997.
25. Vaca, A. and D.L. Kunze. Depletion of intracellular Ca^{2+} stores activates a Ca^{2+} -selective channel in vascular endothelium. *Am. J. Physiol.* 267: C920-C925, 1994.
26. van Breemen, C., Q. Chen and I. Laher. Superficial buffer barrier function of smooth muscle sarcoplasmic reticulum. *Trends Pharmacol. Sci.* 16: 98-105, 1995.
27. Willmott, N.J., Q. Choudhury and R.J. Flower. Functional importance of the dihydropyridine-sensitive, yet voltage-insensitive store-operated Ca^{2+} influx of U937 cells. *FEBS Lett.* 394: 159-164, 1996.
28. Wu, S.N., C.R. Jan and H.F. Li. Characteristics of store-operated Ca^{2+} -permeable current in monocytic U937 cells. *Chin. J. Physiol.* 40: 115-120, 1997.
29. Wu, S.N., T.L. Hwang, C.R. Jan and C.J. Tseng. Ionic mechanisms of tetrandrine in cultured rat aortic smooth muscle cells. *Eur. J. Pharmacol.* 327: 233-238, 1997.
30. Zweifach, A. and R.S. Lewis. Rapid inactivation of depletion-activated calcium current (I_{CRAC}) due to local calcium feedback. *J. Gen. Physiol.* 105: 209-226, 1995.